

Iron Removal as Goethite from Synthetic Laterite Leach Solutions

Goutam Kumar Das* and Jian Li

Cite This: *ACS Omega* 2023, 8, 11931–11940

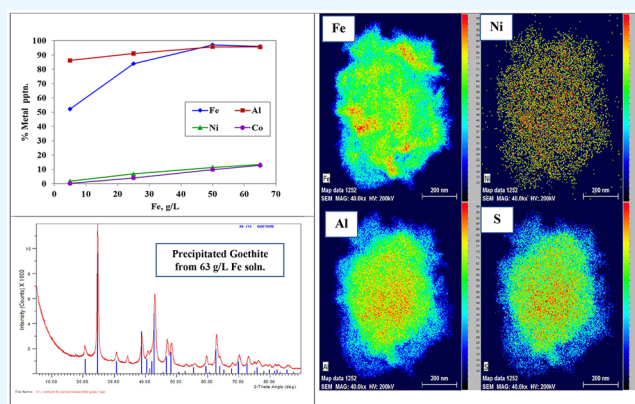
Read Online

ACCESS |

Metrics & More

Article Recommendations

ABSTRACT: The aim of this study was to precipitate goethite from high-iron(II)-bearing atmospheric and heap leach solutions of lateritic nickel ore generated either by reductive leaching of the ore or by reducing Fe(III) of the leach solution to Fe(II) using a suitable reducing agent and to understand the Ni and Co losses during the iron precipitation. Removal of Fe was carried out using an oxidative hydrolysis technique targeting goethite precipitation from a synthetic laterite leach solution containing Fe as ferrous (Fe(II)), Al, Mg, Ni, Co, Cr, Mn, Cu, and Zn using limestone as the neutralizing agent and air as an oxidant. The behavior of goethite precipitation and the losses of Ni and Co were examined under various conditions of pH, temperature, and Fe concentration. The precipitation of Fe increased with increasing pH, temperature, and feed Fe(II) concentration. Precipitation at pH ~4.0–4.1 (measured at ambient temperature) and 90 °C resulted in ~96–97% Fe removal from a feed solution containing more than 50 g/L Fe(II), giving ~1 g/L Fe in the final liquor. Goethite formation was confirmed as a result of the Fe precipitation, and it appeared to take place via ferrihydrite/schwertmannite intermediate phases. The crystallinity of the goethite increased with time, temperature, and feed Fe(II) concentration. The goethite precipitate was found to be associated with an alunite phase. Losses of Ni and Co during Fe precipitation increased with pH, temperature, and feed Fe(II) concentration. The losses were significant above pH 4 and found to be ~7–22% Ni and 4–19% Co in the pH range 4.1–5. The test results indicate that efficient Fe removal via goethite precipitation can be achieved from reduced atmospheric and heap leach solutions of laterite ore; however, careful pH control is required to minimize the loss of Ni and Co during this precipitation.



1. INTRODUCTION

Nickel laterite processing through high-pressure acid leaching (HPAL) is a standard technology where most of the iron from the ore is dissolved and rejected *in situ*, often as hematite^{1,2} and jarosite.² Compared to HPAL, atmospheric acid leaching (AL) and heap leaching (HL) of laterites only dissolve the ore,^{3–5} giving much higher levels of solution impurities, mainly iron.^{6,7} Commercially viable techniques to effectively remove such high iron levels from AL and HL solutions with minimum loss of valuable metals have yet to be established for these processes as independent AL and HL operations.

Several iron removal processes have been developed since the first application of jarosite precipitation⁸ within the zinc industry in the early 1960s. These include the goethite,⁹ jarosite,¹⁰ para-goethite,^{11–13} and hematite¹⁴ processes. The hematite process mainly operates at high temperature^{15,16} and therefore is not suitable for low-temperature (<100 °C) application. The jarosite process has been applied successfully in the zinc industry and other base metal industries for many years⁸ but has become increasingly unpopular due to environmental concerns over producing large volumes of

unstable acid-generated waste.^{13,17} The para-goethite process is also well established in the zinc industry, being used by Zincor, South Africa, and Nyrstar (previously Zinifex), Australia; however, this process is similar to the jarosite process, as it produces large volumes of sulfate-bearing sludge^{11,13} that can represent an environmental threat.

The goethite process was reported in early publications by Davey and Scott,⁹ Dutrizac⁸ and Boxall et al.,¹⁸ where it was proposed that iron could be precipitated as “goethite” by either oxidation or dilution methods. In the dilution method, Fe(III) present in leach solution was added to a precipitation tank at such a rate that the Fe(III) concentration was maintained at less than 2 g/L during precipitation. Roche¹⁹ patented an iron removal process using this method and claimed goethite

Received: November 28, 2022

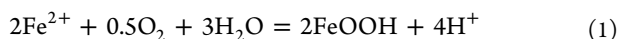
Accepted: March 15, 2023

Published: March 27, 2023



precipitation from the Fe(III) solutions obtained from atmospheric leaching of laterite ore. Wang et al.²⁰ also studied goethite precipitation from Fe(III) solution using a similar method. Their subsequent mineralogical characterization studies^{20,21} confirmed that iron precipitation was mostly as ferrihydrite and/or schwertmannite, with goethite only present as a minor phase. Ferrihydrite/schwertmannite formation has also been reported during partial neutralization of synthetic pressure acid leach liquor.²² Dousma and Bruyn²³ indicated that conversion of iron hydroxide/ferrihydrite/schwertmannite to goethite is possible under suitable conditions; however, it is normally slow and could take from 8 to 37 h to complete at 90 °C.

The oxidation method represents the oxidative hydrolysis of Fe(II) to form goethite^{18,24} as indicated in the equation



Goethite formation via the oxidation method appears to be a suitable technique for iron removal from reduced AL and HL leach solutions, as it produces less sludge relative to the jarosite and paragoethite processes.³ Literature information on goethite precipitation via an oxidative hydrolysis technique from nickel laterite leach solutions is limited, with only the effect of pH on nickel loss at specific iron concentrations, typically <15 g/L, and temperatures having been reported.^{24–26} The reported iron concentrations are much lower compared to those typically found in any AL and HL leach solutions, which can be higher than 100 g/L in some instances.^{5–7}

This current study is focused on goethite precipitation from synthetically reduced AL and HL solutions via the oxidation method, seeking to examine both iron removal and the nickel and cobalt losses from high-iron-bearing solutions. The effect of pH, temperature, and iron concentration (~6–60 g/L) on the losses of nickel and cobalt during goethite precipitation were investigated. Such a wide iron concentration range should represent the AL and HL leach solutions produced from a variety of nickel laterite ore types, typically where the leach solutions produced under reducing conditions have iron in the liquor mainly as ferrous.^{27,28} The variable nature of the precipitates formed under these conditions is also discussed.

2. RESULTS AND DISCUSSION

Iron removal via goethite precipitation was performed using a synthetic laterite leach solution containing Fe (as Fe(II)), Al, Mg, Ni, Co, Cr, Mn, Cu, and Zn. The intent was to keep all the iron in solution as Fe(II) prior to precipitation by air oxidation. The base level feed solution composition for the parameter variation study was targeted at 25 g/L Fe(II), 10 g/L Al, 10 g/L Mg, 4 g/L Ni, 0.2 g/L Co, 0.5 g/L Cr, 0.5 g/L Mn, and 0.05 g/L each of Cu and Zn. As the feed solution was prepared in separate batches, the analysis of the major elements (Fe, Al, Ni and Mg) in the liquor varied to some extent, whereas variations for minor elements were minimal. The average composition of the feed solution is given in Table 1. For the iron concentration variation study only the Fe(II) concentration was varied, keeping all the other elemental concentrations the same, as shown in Table 1.

Goethite precipitation was carried out by varying the parameters pH, temperature, and liquor Fe(II) concentration. Prior to adding air into the reactor, the solution pH was raised to attain the target precipitation pH using ~12% w/w

Table 1. Synthetic Laterite Leach Solution Composition

feed solution analysis, g/L								
Fe(II)	Al	Ni	Co	Cr	Cu	Zn	Mn	Mg
24.9	10.6	4.1	0.20	0.52	0.06	0.05	0.65	10.2

limestone slurry at the test temperature. While raising the pH, a minor amount of Fe(III) present in the solution was precipitated along with some Al, where the extent of Al precipitation was dependent on the pH of the reaction.

The pH reported in this study is an offline value (room temperature, ~21–22 °C) measured on the filtrate liquor of samples from the reactor. This was considered as a better option to present pH data, due to the drift of online values in the reactor slurry during a test and also between tests. This drift was possibly due to a thin coating of iron precipitate on the surface of the pH electrode that could lead to clogging of the electrode. Based on the offline pH, the online pH was adjusted accordingly during the reaction as required. Such coatings on glass electrodes have also been reported in the goethite precipitation study by Chang et al.,²⁴ where the pH in the reactor was measured with precision pH test paper.

2.1. Effect of pH. The effect of pH on goethite precipitation was studied over the range of 3.5–5.0 for up to 5 h of reaction at 90 °C. The precipitation of Fe increased with time at each pH (Figure 1), where the trend was found to be

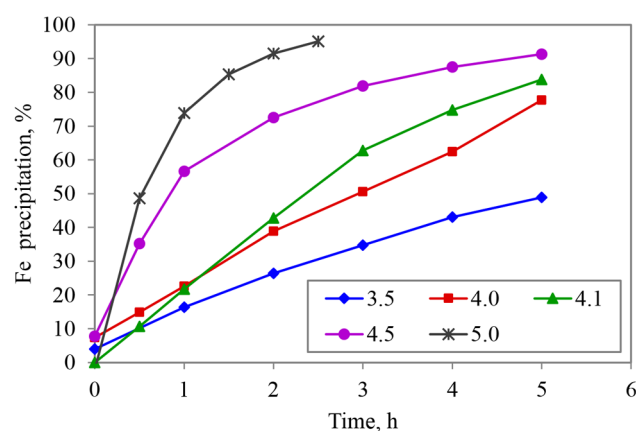


Figure 1. Precipitation behavior of Fe from a synthetic laterite leach solution by oxidative hydrolysis at various pH values (3.5–5.0) and 90 °C.

almost linear for the pH values 3.5, 4.0, and 4.1. The rate of Fe precipitation was lower at pH 3.5 (~31 mg/L/min) compared to the other pH values, giving only 49% precipitation after 5 h. A higher rate of initial Fe precipitation was obtained at pH 4.5 and 5.0 compared to the pH range of 3.5–4.1. The rate was highest (109.8 mg/L/min) at pH 5.0, giving >95% Fe precipitation in 2.5 h, where the Fe concentration in the final liquor was found to be ~0.7 g/L. Chang et al.²⁴ reported a ferrous oxidation rate of 80 mg/L/min from a reduced laterite leach solution containing 14 g/L Fe and 0.63 g/L Ni for goethite precipitation at pH 4–6, where <0.3 g/L Fe in the solution was achieved after 3 h. Therefore, higher pH leads to faster Fe(II) oxidation and goethite precipitation; however, this also has an impact on the losses of Ni and Co.

Figure 2 indicates a significant portion of the Al precipitated while attaining the target pH prior to air addition for oxidative

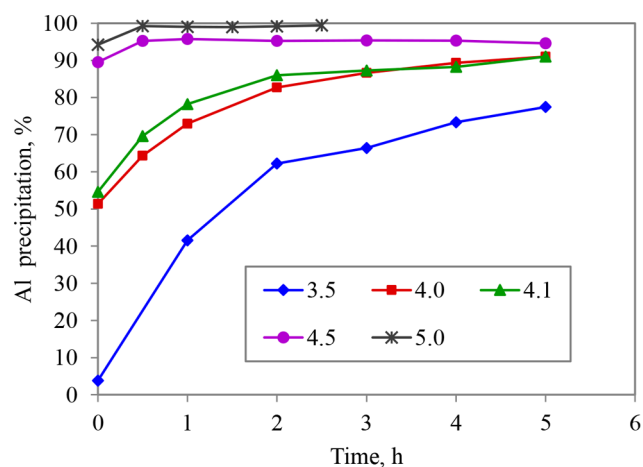


Figure 2. Precipitation behavior of Al from a synthetic laterite leach solution during oxidative hydrolysis of Fe(II) at various pHs (3.5–5.0) and 90 °C.

hydrolysis of Fe(II). Almost 50% of the Al precipitated on reaching pH 4.0–4.1, while this increased to 90–95% at pH 4.5–5.0. During Fe removal, the precipitation of Al further increased with increasing time, reaching ~77% and ~91% at pH 3.5 and 4.0–4.1, respectively, after 5 h. The reported Al removal data during goethite precipitation via oxidative hydrolysis from laterite leach solution are limited. However, the behavior of Al precipitation during Fe (Fe(III)) removal from laterite leach solution via the dilution method and its effect on Ni and Co losses have been extensively reported.^{19,22,29,30} Roche¹⁹ noted final liquor Al concentrations of 2.13–2.67 g/L from a feed Al concentration of ~4 g/L during iron removal via the dilution method for various doses of limestone slurry. The present test results clarify that most of the Al can be removed easily by increasing the pH of the liquor to >4; however, this will result in higher Ni/Co losses. Therefore, a second-stage precipitation may be appropriate for complete removal of remaining iron and aluminum at pH >4, where precipitated Ni/Co can be recovered by leaching of the second-stage solid and recycling back the liquor to the first-stage iron removal.

The effect of pH on the losses of Ni and Co during Fe/Al precipitation is discussed in section 3.2.

2.2. Effect of Temperature. The effect of temperature on goethite precipitation was investigated at temperatures of 70, 80, 90, and 97 °C while maintaining the pH at ~4.0–4.1 for 5 h. Figure 3 shows that Fe precipitation increased on raising the temperature from 70 to 90 °C, after which no further increase occurred, whereas Al precipitation decreased with increasing temperature up to 97 °C.

The trend for Ni and Co losses was to increase with temperature; however, these losses were below 8%. Maxima of 7.4% Ni and 5.2% Co losses were obtained at 97 °C, corresponding to analyses of 0.13% Ni and 0.005% Co in the precipitated solid. The effect of temperature on zinc loss from 30 g/L Fe(II) solutions containing 15 g/L Zn have been reported by Davey and Scott⁹ for goethite precipitation in the temperature range of 65–95 °C. The Zn analysis in the precipitated solid increased from 0.61% to 1.11% with an increase in temperature from 65 to 95 °C, respectively. This is also consistent with the valuable metals' loss being expected to

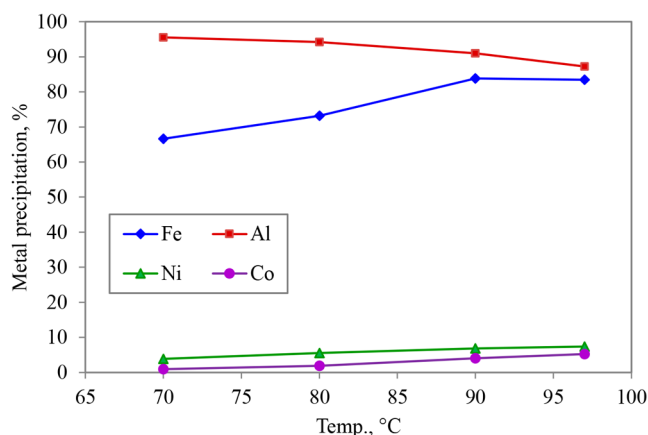


Figure 3. Effect of temperature on metal precipitation from synthetic laterite leach solution by oxidative hydrolysis at pH 4.0–4.1 after 5 h.

increase during goethite precipitation with an increase in temperature.

2.3. Effect of Fe Concentration. The effect of varying Fe(II) concentrations between 6 and 65 g/L was examined at pH 4.0–4.1 and 90 °C over a 5 h period. The highest Fe concentration actually achieved was 63.2 g/L, due to the common (sulfate) ion effect from the high Al and Mg concentrations in the liquor (10 g/L each) and since the free acidity was low (<5 g/L).

Precipitation increased with Fe concentration up to 50 g/L, after which no further increase was observed (Figure 4). For

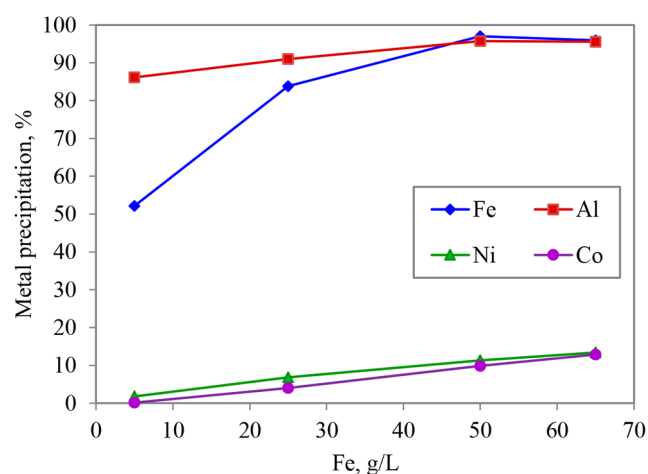


Figure 4. Effect of Fe(II) concentration on metal precipitation from a synthetic laterite leach solution by oxidative hydrolysis at pH 4.0–4.1 and 90 °C after 5 h.

the Fe feed concentration range 50–63 g/L, Fe precipitation was ~96–97%, resulting in ~1 g/L Fe in the final liquor. Significant Al precipitation (~86%) occurred at a low feed Fe concentration (6 g/L), where Fe precipitation was ~52% after 5 h of reaction. Chang et al.²⁴ reported >95% Fe precipitation after a 4 h reaction from a leach solution containing 14 g/L Fe. This suggests that a high Al concentration in the liquor has an impact on goethite precipitation at low Fe concentration. The extent of Al precipitation gradually increased with Fe concentration up to 50 g/L, after which no further increase took place.

Table 2. Analyses of the GSW and DIW Solids for the Tests with Feed Fe Concentrations of 6 and 63 g/L

feed liquor Fe concn (g/L)	solid analysis, %									
	Fe	Al	Ni	Co	Ca	S	Cr	Cu	Mn	Mg
6 (GSW)	2.6	7.00	0.053	0.000	15.1	15.3	0.34	0.010	0.001	0.001
63 (GSW)	13.7	2.34	0.142	0.006	15.5	13.6	0.12	0.012	0.005	0.001
6 (DIW) ^a	7.6	20.2	0.148	<0.002	0.1	6.9	0.99	0.030	0.003	0.003
63 (DIW) ^a	44.1	7.05	0.415	0.018	<0.002	3.1	0.36	0.035	0.015	0.003

^aValues for Cr, Cu, Mn, and Mg are calculated values based on the unwashed solid analysis of these elements.

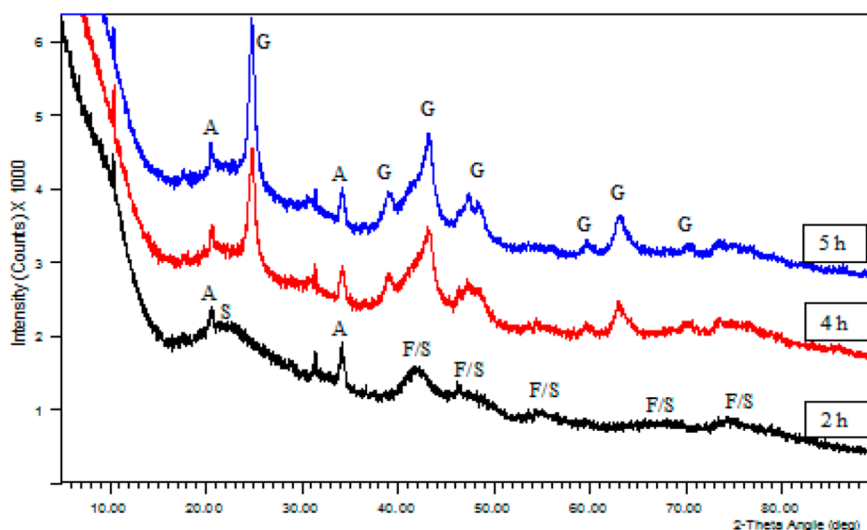


Figure 5. XRD traces of the 2, 4, and 5 h precipitates from the test with 25 g/L feed Fe concentration at pH 4.1 and 90 °C. Mineral phases: G = goethite, F = ferrihydrite, S = schwertmannite, and A = alunite.

Figure 4 shows near-linear losses of Ni and Co with an increase in feed Fe concentration, giving up to ~13% Ni and Co losses at 63 g/L Fe. The Ni loss was generally slightly higher compared to that of Co. Davey and Scott⁹ attempted goethite removal from a high Fe (75 g/L Fe(II)) and Ni (40 g/L) chloride solution at pH 3.5, reporting a much higher Ni loss, which they concluded was due to the high Ni concentration in the feed liquor.

The precipitated solid was washed with gypsum-saturated water (GSW) to retain the calcium sulfate present in the solid, and where required, GSW-washed solid was further washed with DI water (DIW) for removal of calcium sulfate from the solid. The analyses of GSW-washed and DIW-washed (for complete Ca washing) solids from the tests for feed Fe concentrations of 6 and 63 g/L are given in Table 2. The GSW-washed precipitate contained a significant amount of gypsum ($\text{CaSO}_4 \cdot 2\text{H}_2\text{O}$) that was confirmed by XRD analysis and high Ca (~15%) and S (~14–15%) analyses in the solid. Once the gypsum was completely removed by DIW washing, the contents of the other elements increased ~3 times. The S analyses in the DIW solids were high (~3–7%); the reason for high S (as sulfate) retention in the DIW-washed solids is discussed in the next section.

3. PRECIPITATED SOLID CHARACTERIZATION AND NI/CO LOSSES

3.1. Precipitate Characterization. The characterization of precipitated solids was carried out by X-ray diffraction (XRD) and transmission electron microscopy (TEM) analyses using the DIW-washed solids. The XRD traces of the 2, 4, and 5 h solids from tests with 25 g/L Fe feed concentration at pH

4.1 and 90 °C are given in Figure 5. The trace for the 2 h solid mostly consists of broad peaks, indicating the poorly crystalline nature of the precipitate. A prominent broad peak after 40° (2θ angle) is due to ferrihydrite/schwertmannite phases. Therefore, ferrihydrite/schwertmannite formation occurs at the early stages of the oxidative hydrolysis reaction of iron precipitation. The XRD traces for the 4 and 5 h solids confirmed goethite peaks in the precipitate, and goethite crystallinity was found to increase with time. Thus, it appears that schwertmannite and/or ferrihydrite formation is a precursor for goethite formation, as discussed later. The formation of an alunite phase was also identified.

For additional confirmation of the phases formed, TEM images and selected area electron diffraction (SAED) patterns of the 2 and 5 h precipitates are given in Figure 6. The morphologies of 2 and 5 h solids are very similar; however, SAED of the 2 h sample shows mostly rings at *d* spacings of 0.25 and 0.147 nm. This confirms the presence of either poorly crystalline ferrihydrite and/or schwertmannite; both have *d* spacings close to these values. SAED of the 5 h sample is consistent with the presence of goethite. The *d* spacings in nm are labeled for the SAED rings to indicate ferrihydrite (top right) and goethite (bottom right) in Figure 6. This confirms the XRD findings of conversion of a poorly crystalline iron oxide/hydroxide based precipitate to goethite with time. The Fe(II)-catalyzed transformation of ferrihydrite to goethite and hematite/maghemite has been reported.^{31–33} Goethite formation from ferrihydrite is mainly thought to occur through dissolution/reprecipitation and surface complexation mechanisms.^{32,34}

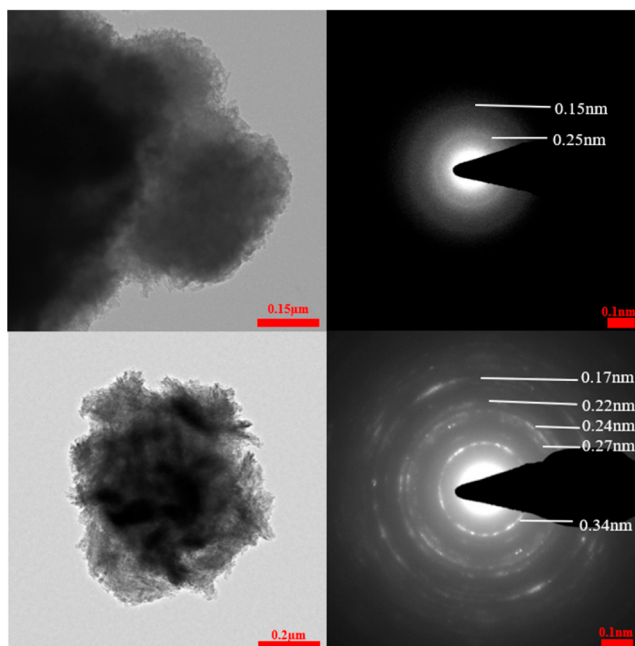


Figure 6. TEM and SAED images of 2 h (top images) and 5 h (bottom images) precipitates from the test with 25 g/L feed Fe concentration at pH 4.1 and 90 °C. The d spacings in nm are labeled for the ferrihydrite (top right) and goethite (bottom right) phases.

Andreeva et al.³⁵ reported goethite formation from ferrihydrite through its dissolution and reprecipitation. Andreeva et al.³⁶ also proposed a different mechanism in their earlier study of oxidative Fe(II) hydrolysis based on the concept of surface adsorption of Fe(II) ion on the Fe(III) hydroxide surface. In this mechanism, the oxygenated Fe(II) species $[\text{Fe}^{2+}\cdot\text{O}_2]$ is adsorbed on the surface of $\text{Fe}(\text{OH})_2^+$ species, where the $\text{Fe}(\text{OH})_2^+$ species is formed by the initial oxidation of Fe(II) to Fe(III), followed by partial hydrolysis. The $[\text{Fe}^{2+}\cdot\text{O}_2]$ species adsorbed on the $\text{Fe}(\text{OH})_2^+$ surface undergoes dehydroxylation to aggregate the building blocks of the goethite structure.

Published sulfur (S) analysis data for goethite solids precipitated from sulfate systems is limited. Chang et al.²⁴

and Yue et al.²⁵ reported the formation of goethite in the studies from synthetic and laterite leach solutions containing Fe(II); however, they did not report S analysis within the goethite solids. The presence of S in the DIW solids of this study was mostly from the presence of an alunite phase and may be partially due to a schwertmannite phase. The S analyses for the 2, 4, and 5 h solids were 6.1, 5.5 and 5.1%, respectively.

A significant sulfate contamination (8.8–13.8%) in the goethite precipitate was reported by Davey and Scott.⁹ They indicated that the sulfate contamination was due to the possible formation of basic sulfates; however, they did not mention ferrihydrite/schwertmannite formation during goethite precipitation. This may reflect the limited resolution of available XRD instruments at the time of their research compared to modern instruments. Liu et al.³⁷ reviewed the surface adsorption of goethite and claimed that goethite can have a very active surface to adsorb various anions including sulfate. As the 5 h solid was found to contain ~5.1% S (equivalent to 15% sulfate), it is expected that a portion of the S is due to sulfate adsorption on the goethite surface. However, the formation of alunite and schwertmannite phases will contribute to the majority of the S present in the precipitated solids.

A comparison of the XRD traces for the 5 h solids formed at 70, 90, and 97 °C is given in Figure 7. This shows that the precipitate formed at 70 °C was poorly crystalline, being mostly composed of ferrihydrite/schwertmannite and alunite phases. A higher temperature is required to promote goethite formation from the oxidative hydrolysis of Fe(II) and, given the sharpening of peaks, the crystallinity of the goethite increased with the increase of temperature.

To compare the mineralogy of the precipitates formed at various Fe concentrations, XRD traces of the 5 h solids from the 6, 25, and 63 g/L Fe(II) tests are presented in Figure 8. The mineralogical analysis of Fe precipitate formed at a low Fe(II) concentration (~6 g/L) was significantly different compared to the precipitates formed at higher concentrations. The presence of goethite cannot be positively identified in the precipitate formed from the 6 g/L Fe(II) test. An alunite phase was found instead, while schwertmannite and ferrihydrite were also expected to form, as ~52% Fe precipitated during the

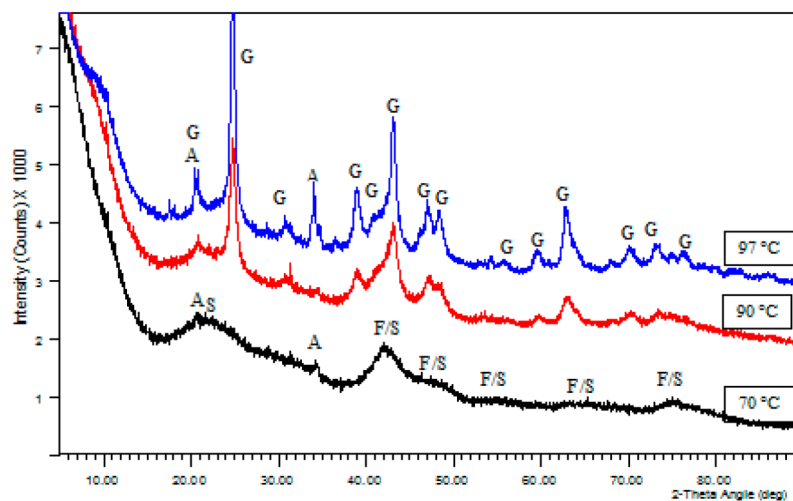


Figure 7. XRD traces for the 5 h precipitates from tests conducted at 70, 90, and 97 °C with 25 g/L feed Fe concentration at pH 4.1. Mineral phases: G = goethite, F = ferrihydrite, S = schwertmannite, and A = alunite.

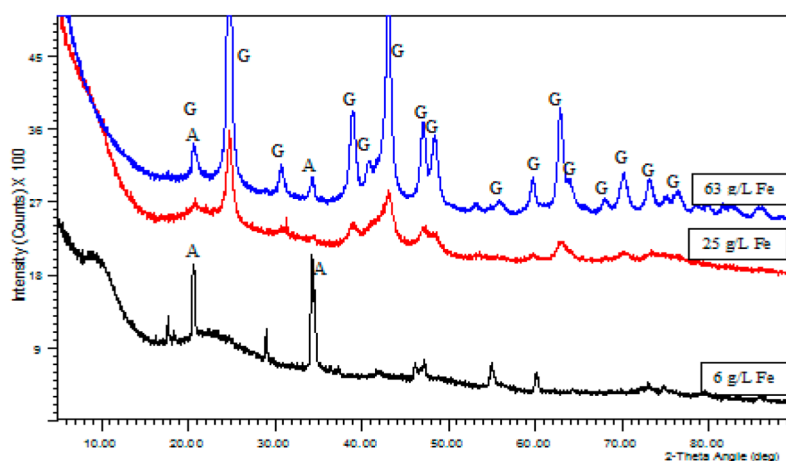


Figure 8. XRD for the 5 h precipitates from tests conducted with 6, 25, and 63 g/L Fe(II) at pH 4.1 and 90 °C. Mineral phases: G = goethite and A = alunite.

Table 3. Ni and Co Losses to, and Contents in, Precipitated Solids Formed during Iron Removal from 25 g/L Fe(II) feed solution at Various pH Values during the Oxidative Hydrolysis of Synthetic Laterite Solution

element	metal loss, %					precipitate analysis, %				
	pH = 3.5	pH = 4.0	pH = 4.1	pH = 4.5	pH = 5.0	pH = 3.5	pH = 4.0	pH = 4.1	pH = 4.5	pH = 5.0
Ni (0 h)	0.0	0.3	0.3	0.7	1.5	0.003	0.012	0.014	0.024	0.047
Ni (final)	1.1	4.2	6.8	10.6	22.0	0.032	0.095	0.128	0.186	0.390
Co (final)	0.7	2.3	4.0	8.6	18.8	0.001	0.003	0.004	0.007	0.016

reaction. In comparison, Yue et al.²⁵ confirmed goethite formation in their study from a solution containing ~ 5.6 g/L Fe(II) and 10 g/L Ni. This suggests that the presence of Al affected goethite formation, as well as overall Fe removal. Figure 8 shows that goethite crystallinity increased significantly at higher Fe(II) concentration in the feed solution.

3.2. Nickel and Cobalt Losses. Losses of Ni and Co are an issue during Fe removal from laterite leach solutions, and this imposes limitations on the Fe removal process conditions to minimize the valuable metal losses. Such losses are generally expected to increase with pH during Fe and Al precipitation, and this trend was also found in this study (Table 3). The Ni and Co losses at pH 3.5 were low ($\sim 1\%$); however, these increased rapidly after pH 4.1, giving ~ 9 – 11% and ~ 19 – 22% losses at pH 4.5 and 5.0, respectively. The loss of Co was lower than that of Ni, which is possibly due to the much lower Co concentration (0.2 g/L Co against ~ 4 g/L Ni) in the feed liquor.

Chang et al.²⁴ reported 4.1–15.9% Ni loss within the pH range 2.5–4.0 from laterite leach solutions. In the present study, the Ni and Co losses at pH 4.0–4.1 were found to be ~ 4 – 7% , where the extents of Fe and Al precipitation were ~ 78 – 84% and $\sim 91\%$, respectively, from a feed solution containing ~ 25 g/L Fe. A similar Ni loss of $\sim 5.6\%$ has been reported by Yue et al.²⁵ in the pH range 3.9–4.3 from a low Fe(II) synthetic feed solution having ~ 5.6 g/L Fe and 10 g/L Ni. However, they achieved precipitation using H_2O_2 instead of air/oxygen, and the reaction was completed within 45 min, the solid formed having a high Ni content of 5.37%.

The analyses of Ni and Co in the final solids (washed with GSW) at pH 4.0–4.1 were 0.095–0.128% and 0.003–0.004%, respectively (Table 3). The Ni analysis is low in the precipitated solid due to the presence of a significant amount of gypsum (~ 65 – 70%). Once the gypsum dissolved with DIW washing, the solid reported approximately 3-fold higher Ni and

Co analyses in the precipitate, at ~ 0.27 – 0.36% and 0.012%, respectively. A similar Ni analysis (0.467%) was reported by Chang et al.²⁴ at pH 3–4. A comparison of Ni loss data from various published iron precipitation studies is given in Table 4. This shows that Ni loss is dependent on the pH irrespective of the adopted precipitation method and that a lower pH is beneficial to minimize the Ni loss during Fe removal from laterite solution. Therefore, based on the atmospheric leaching technique adopted for the laterite ore with or without reducing agents, a suitable Fe removal route can be chosen depending on the Fe(II) or Fe(III) concentration in the liquor. The oxidative hydrolysis route for Fe(II) will generate crystalline goethite during Fe removal, which should give better filtration or solid–liquid separation characteristics compared to the formation of paragoethite (i.e., ferrihydrite/schwertmannite) that will be produced from Fe(III) via the dilution or normal Fe(III) precipitation methods.

The loss of Ni was also found to increase in this study with increasing temperature and feed Fe(II) concentration (Figures 3 and 4). Figure 9 shows the Ni loss behavior with time from the feed Fe(II) concentration variation tests. The maximum Ni loss of 13.4% was obtained for 63 g/L Fe(II) feed (Fe/Ni ratio 15.6) under the conditions of 90 °C and pH 4.0–4.1. The Ni analyses were 0.142% and 0.415% for the GSW and DIW washed solids, respectively (Table 2).

Yue et al.²⁵ claimed that Ni loss took place through surface adsorption onto goethite and incorporation into the goethite lattice. They also proposed a mechanism of goethite formation with Ni incorporation and suggested that Ni(II) ions enter into the goethite lattice in place of Fe(III) due to the similar ionic radii of Ni(II) and Fe(III). The adsorption of Ni on different goethite surfaces was studied by Beukes et al.,³⁸ who described an increase of adsorption with pH (>3) where the extent of adsorption depended on the goethite surface area.

Table 4. Comparison of Various Iron Precipitation Reactions and Associated Ni Loss Data from Published Studies

feed liquor		precipitation conditions				Ni analysis in the solid, %			precipitation route	ref
Fe, g/L	Ni, g/L	solution type	neutralizing agent	pH	Temp, °C	Fe precipitation, %	Ni loss, %			
28.0	4.7	synthetic	limestone	2.0	85	87.92	0.19	0.0079	dilution method (mainly paragoethite)	20 ^d
89.1	4.74			4.0	85	96.17	19.17	0.166		
30.0	5.1	synthetic	limestone	3.0	85	91.5	2.35	0.06	dilution method (mainly paragoethite)	37 ^b
				4.0	85	95.4	11.7	0.27		
27.8	4.36		limestone	2.0	85	~93 ^d	0.2	0.0015	dilution method (mainly paragoethite)	19 ^c
26.7	3.96			3.0	85	100 ^d	17.5	0.28		
125	NR	laterite tank leach	limestone	3.2 (stage 1)	NR	98	1.3	NR	ferric hydroxide (paragoethite type)	5
				4.7 (stage 2)	NR	99 ^d	2.1	NR		
~5.6	~10	synthetic	NaOH	2.0–2.3	85	14.5	0.11	0.56	oxidative hydrolysis using H ₂ O ₂ (mainly goethite)	25
				2.4–2.8		98.63	0.26	0.28		
				2.9–3.3		99.84	1.05	1.13		
				3.4–3.8		100	1.99	2.17		
				3.9–4.3		100	5.59	5.37		
14	0.63	reduced limonite leach	basic MgCO ₃	2.5–3.0	95	96.8 ^d	4.12	0.112	oxidative hydrolysis using air (mainly goethite)	24
				3.0–4.0		97.4 ^d	15.9	0.467		
23.3	4.1	synthetic reduced laterite soln	limestone	3.5	90	49.8	1.1	0.032	oxidative hydrolysis using air (mainly goethite)	this work ^e
				4.0		77.7	4.2	0.095		
25.4	4.0			4.1		83.8	6.8	0.128		
23.3	4.1			4.5		91.3	10.6	0.186		
				5.0		95.1	22	0.390		
50.1	4.0			4.1		97.1	11.4	0.135		

^aTest no. FFD-3 and FFD-5 of cited reference. ^bTest no. FNA-3 and FNA-4 of cited reference. ^cExamples 1 and 2 of cited reference. NR denotes not reported. ^dApproximately calculated values based on the available data in the corresponding reference. ^eReported pH is the solution pH measured at ambient temperature.

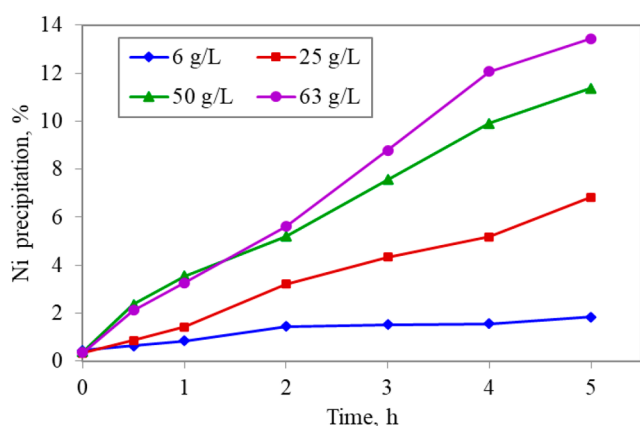


Figure 9. Behavior of Ni loss during iron precipitation for different feed Fe(II) concentrations at pH 4.0–4.1 and 90 °C.

Elemental mapping from the TEM/EDS analysis of the particle shown in the bottom images of Figure 6 is presented in

Figure 10. This shows an even distribution of Ni in the particle, which suggests that Ni loss occurs through both surface adsorption and incorporation into the goethite structure. However, the possibility of some Ni coprecipitation cannot be eliminated, especially at high feed Fe(II) concentrations. The distributions of Al and S were similar, and this is consistent with the copresence of an alunite phase with the goethite solid.

4. CONCLUSIONS

Goethite precipitation from synthetic laterite leach solution resulted in increasing Fe removal with increasing pH, temperature, and feed Fe(II) concentration. The extent of Al precipitation also increased with increasing pH and feed Fe(II) concentration but decreased with temperature. The final Fe concentration was ~1 g/L when the feed Fe(II) concentration was above 50 g/L. During the early stage of the reaction, the Fe precipitate was poorly crystalline due to the formation of ferrihydrite/schwertmannite phases; however, after 2 h of reaction goethite formation had commenced and its crystallinity increased with time. Therefore, goethite formation

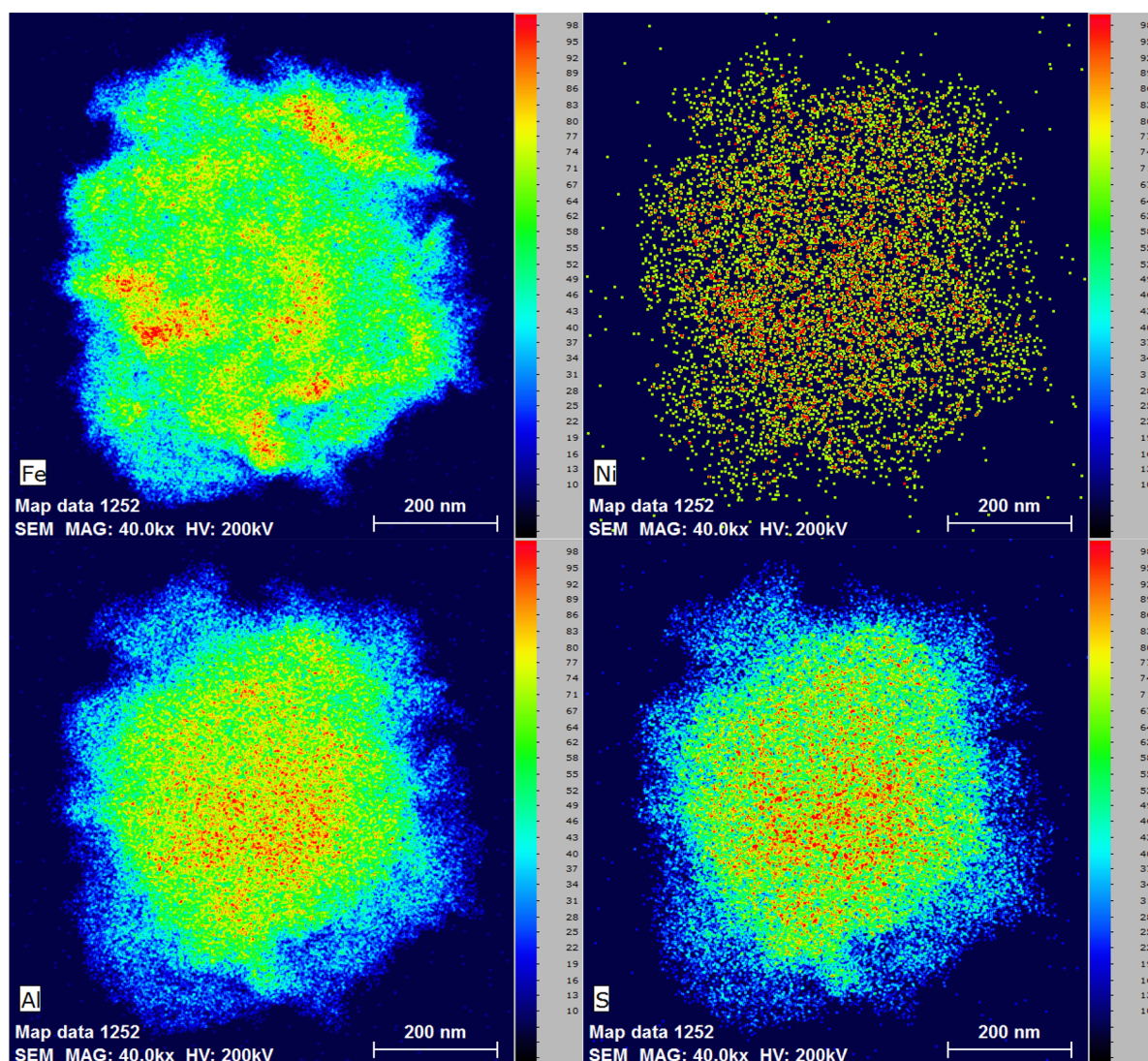


Figure 10. Elemental mapping from the TEM/EDS analysis of a particle in the 5 h precipitate from the test with 25 g/L feed Fe concentration at pH 4.1 and 90 °C.

appeared to take place via the ferrihydrite/schwertmannite phases. The crystallinity of the goethite also improved with increases of temperature and feed Fe(II) concentration.

Loss of Ni and Co occurred during Fe precipitation, and the losses increased with pH, temperature, and feed Fe(II) concentration. The Ni and Co losses rose significantly with an increase in pH of above 4 and were found to be ~7–22% Ni and 4–19% Co in the pH range of pH 4.1–5. Careful pH control at ≥ 4 will minimize the Ni and Co losses during goethite precipitation. Two precipitation stages will likely be a better option for high-Fe(II)-bearing leach liquor for goethite precipitation to minimize Ni/Co losses from laterite leach solution.

5. EXPERIMENTAL SECTION

5.1. Goethite Precipitation. The goethite precipitation study was carried out with a synthetic solution prepared using laboratory reagent grade and analytical reagent grade sulfate salts of ferrous iron, aluminum, nickel, cobalt, magnesium, chromium, manganese, zinc, and copper. The required amounts of metal sulfate salts were dissolved in DI water in the presence of a small quantity of sulfuric acid to minimize

Fe(II) oxidation and precipitation. To prevent the oxidation of Fe(II) during storage, a small amount of sulfur dioxide gas was prepurged through the solutions.

Tests were carried out in a 2 L capacity continuously stirred, baffled glass reactor having a flat flange/multisocket lid fitted with pH probe, thermometer, air purging tube, neutralizing agent slurry addition tube, and condenser. The reactor was heated in an oil bath (ULTRAPEG 400) with provision to control the bath temperature to maintain the reactor temperature to within ± 1 °C. The precipitation reaction was carried out by oxidizing Fe(II) using air and adding limestone slurry as the neutralizing agent.

A required amount of test solution was added to the reactor, which was then placed in the oil bath. To prevent Fe(II) oxidation, a nitrogen blanket was maintained in the reactor headspace prior to air addition. After attaining the test temperature, limestone slurry (pulp density $\sim 12\%$ w/w) was slowly placed in the reactor to achieve the target precipitation pH. Once the reactor pH was reached, a sample was collected and air was employed at a flow rate of ~ 2.5 L/min. The reactor pH was maintained by adding limestone slurry, typically in a continuous mode, using a peristaltic pump. Reactions were

carried out for 5 h by varying pH, temperature, and feed Fe(II) concentration. Slurry samples from the reactor were collected at 0.5 and 1 h and subsequently at hourly intervals. The collected samples were filtered immediately, and the solid was washed thoroughly with GSW and dried overnight in an oven at ~80 °C. Elemental analyses for both the liquors and solids were performed using an ICP-OES instrument adopting standard procedures.

All the tests were performed by conducting both physical mass balance (based on liquor and solids/slurry output/input \times 100) and elemental mass balance (elemental mass output/input \times 100). The baseline test performed with 25 g/L Fe concentration was repeated twice to verify the reproducibility of the test data.

Since limestone slurry was used as the neutralizing reagent, gypsum formation took place during iron precipitation. The amount of gypsum in the precipitated solid was ~67–70% w/w in this study. Therefore, precipitated solids selected for characterization studies were washed thoroughly with DIW to remove the gypsum (until the wash water was found to be sulfate free by testing with barium chloride solution).

5.2. Instrumental Techniques. The samples for X-ray diffraction (XRD) analysis were air-dried, finely ground, and back-pressed into conventional XRD sample holders. XRD measurements were carried out using a PANalytical high-resolution multipurpose powder diffractometer (Empyrean) with Co K α radiation and operating at 45 kV and 40 mA. A Bragg–Brentano high-definition monochromator was used in front of the incident beam. A PIXcel3D proton-counting X-ray detector was used to collect the data over an angular range of 10–90° 2 θ in continuous scan mode for 1 h. The XRD data was interpreted with XPLOR and HighScore Plus (3.04) software using the ICDD and ICSD databases.

The samples for transmission electron microscopy (TEM) analysis were suspended in water and deposited on standard perforated carbon support films on copper grids. TEM imaging and elemental analyses were performed using a FEI TALOS field-emission-gun transmission electron microscope (FEG-TEM) Titan G2 80-200 TEM/STEM with ChemiSTEM technology, equipped with an energy dispersive X-ray spectrometer (EDS) and selected area electron diffraction (SAED) capabilities.

AUTHOR INFORMATION

Corresponding Author

Goutam Kumar Das – CSIRO Mineral Resources Perth, Processing Program, Waterford, Western Australia 6152, Australia; orcid.org/0000-0001-8774-4333; Phone: +61 8 9334 8933; Email: Goutam.Das@csiro.au; Fax: +61 8 9334 8001

Author

Jian Li – CSIRO Mineral Resources Perth, Processing Program, Waterford, Western Australia 6152, Australia

Complete contact information is available at:
<https://pubs.acs.org/10.1021/acsomega.2c07595>

Author Contributions

G.K.D and J.L. made equal contribution to this work.

Notes

The authors declare no competing financial interest.

ACKNOWLEDGMENTS

The authors wish to thank Milan Chovancek and Tuyen Pham for performing chemical analysis, Sophia Surin for collecting the XRD data, and Martin Saunders for the TEM images. The authors also thank Robbie McDonald and Phillip Fawell for reviewing this paper.

REFERENCES

- (1) Liu, K.; Chen, Q.; Hu, H.; Yin, Z.; Wu, B. Pressure acid leaching of a Chinese laterite ore contacting mainly maghemite and magnetite. *Hydrometallurgy* **2010**, *104*, 32–38.
- (2) Whittington, B. I.; Muir, D. M. Pressure acid leaching of nickel laterites: a review. *Miner. Process. Extr. Metall. Rev.* **2000**, *21*, 527–599.
- (3) McDonald, R. G.; Whittington, B. I. Atmospheric acid leaching of nickel laterites review Part I. Sulphuric acid technologies. *Hydrometallurgy* **2008**, *91*, 35–55.
- (4) Watling, H. R.; Das, G. K.; Elliot, A. D.; Li, J.; McDonald, R. G.; Robinson, D. J. Process options for difficult arid-region nickel laterites. In *XXV International Mineral Processing Congress (IMPC)*; Australasian Institute of Mining and Metallurgy: 2010; pp 417–428.
- (5) Willis, B. Atmospheric tank leach flowsheet development for the Caldag nickel project in Western Turkey. In *ALTA Nickel-Cobalt-Copper Conference*; ALTA Metallurgical Services: 2014; pp 66–78.
- (6) MacCarthy, J.; Addai-Mensah, J.; Nosrati, A. Atmospheric acid leaching of silicious goethitic Ni laterite ore: Effect of solid loading and temperature. *Miner. Eng.* **2014**, *69*, 154–164.
- (7) Kittelty, D. A. Low Eh leach with sulphur recycle. International Patent Application WO2008/138038 A1; Nov. 2008.
- (8) Dutrizac, J. E. An overview of iron precipitation in hydrometallurgy. In *International Symposium - Crystallization and Precipitation*; Strathdee, G. L., Klein, M. O., Melis, L. A., Eds.; Pergamon Press: 1987; pp 259–283.
- (9) Davey, P. T.; Scott, T. R. Removal of iron from leach liquors by goethite process. *Hydrometallurgy* **1976**, *2*, 25–33.
- (10) Dutrizac, J. E. Physical chemistry of iron precipitation in the zinc industry. In *Lead-Zinc-Tin'80, (TMS-AIME): Proceedings of a World Symposium on Metallurgy and Environmental Control*; Cigan, J. M., Mackey, T. S., O'Keefe, T. J., Eds.; Metallurgical Society of AIME: 1980; pp 532–564.
- (11) Loan, M.; Newman, O. M. G.; Cooper, R. M. G.; Farrow, J. B.; Parkinson, G. M. Defining the paragoethite process for iron removal in zinc hydrometallurgy. *Hydrometallurgy* **2006**, *81* (2), 104–129.
- (12) Loan, M. *Paragoethite Process: Fundamentals of ferrihydrite, schwertmannite and goethite precipitation*. Ph.D Thesis, Curtin University of Technology, 2004.
- (13) Claassen, J. O.; Meyer, E. H. O.; Rennie, J.; Sandenbergh, R. F. Iron precipitation from zinc-leach solutions: defining the Zincor Process. *Hydrometallurgy* **2002**, *67* (1–3), 87–108.
- (14) Cheng, T. C.; Demopoulos, G. P.; Shibachi, Y.; Masuda, H. The precipitation chemistry and performance of the Akita hematite process -An integrated laboratory and industrial scale study. In *Hydrometallurgy 2003 - Fifth International Conference - Electrometallurgy and Environmental Hydrometallurgy*; Young, C., Alfantazi, A., Anderson, C., James, A., Dreisinger, D., Harris, B., Eds.; Wiley-TMS: 2003; Vol. 2, pp 1657–1674.
- (15) Tozawa, K. Effect of coexisting sulphates on precipitation of ferric oxide from ferric sulphate solutions at elevated temperatures. In *Iron Control in Hydrometallurgy*; Dutrizac, J. E., Monhemius, A. J., Eds.; Ellis Horwood: 1986; pp 455–476.
- (16) McCarthy, F.; McDonald, R.; Woodbridge, G.; Brock, G.; Robinson, D. Iron hydrolysis in the Direct Nickel process. In *IMPC 2016 - XXVIII International Mineral Processing Congress Proceedings - 4th International Symposium on Iron Control in Hydrometallurgy*; Canadian Institute of Mining Metallurgy and Petroleum: 2016; pp 500–520.
- (17) Dutrizac, J. E.; Jambor, J. L. Jarosites and their application in hydrometallurgy. *Rev. Mineral. Geochim.* **2000**, *40*, 405–452.

- (18) Boxall, J. M.; Litz, L. M.; Weise, M. K. Oxygen reactor for the goethite-zinc leach residue process. *J. Met.* **1984**, *36* (8), 58–61.
- (19) Roche, E. G. Iron precipitation. International Patent Application WO/2009/155651 A1; 2009.
- (20) Wang, K.; McDonald, R. G.; Browner, R. E. The effects of iron precipitation upon nickel losses from synthetic atmospheric nickel laterite leach solutions: Statistical analysis and modelling. *Hydrometallurgy* **2011**, *109*, 140–152.
- (21) Wang, K.; Li, J.; McDonald, R. G.; Browner, R. E. Characterisation of iron-rich precipitates from synthetic atmospheric nickel laterite leach solutions. *Miner. Eng.* **2013**, *40*, 1–11.
- (22) Faris, N.; Fischmann, A. J.; Assmann, S.; Jones, L. A.; Tardio, J.; Madapusi, S.; Grocott, S.; Bhargava, S. A study into the behaviour of nickel, cobalt and metal impurities during partial neutralisation of synthetic nickel laterite pressure leach solutions and pulps. *Hydrometallurgy* **2021**, *202*, 105604.
- (23) Dousma, J.; Bruyn, P. L. Hydrolysis - precipitation studies of iron solutions. I. Model for hydrolysis and precipitation from Fe(III) nitrate solutions. *J. Colloid Interface Sci.* **1976**, *56* (3), 527–539.
- (24) Chang, Y.; Zhai, X.; Li, B.; Fu, Y. Removal of iron from acidic leach liquor of lateritic nickel ore by goethite precipitate. *Hydrometallurgy* **2010**, *101*, 84–87.
- (25) Yue, T.; Han, H.; Sun, W.; Hu, Y.; Chen, P.; Liu, R. Low-pH mediated goethite precipitation and nickel loss in nickel hydrometallurgy. *Hydrometallurgy* **2016**, *165*, 238–243.
- (26) Han, H.; Sun, W.; Hu, Y.; Yue, T.; Wang, L.; Liu, R.; Gao, Z.; Chen, P. Induced crystallisation of goethite precipitate from nickel sulphate solution by limonite seeding. *Hydrometallurgy* **2017**, *174*, 253–257.
- (27) Das, G. K.; de Lange, J. A. B. Reductive atmospheric acid leaching of West Australian smectitic nickel laterite in the presence of sulphur dioxide and copper(II). *Hydrometallurgy* **2011**, *105*, 264–269.
- (28) Senanayake, G.; Das, G. K.; de Lange, A.; Li, J.; Robinson, D. J. Reductive atmospheric acid leaching of lateritic smectite/nontronite ores in H₂SO₄/Cu(II)/SO₂ solutions. *Hydrometallurgy* **2015**, *152*, 44–54.
- (29) Wang, K.; Li, J.; McDonald, R. G.; Browner, R. E. Iron, aluminium and chromium co-removal from atmospheric nickel laterite leach solutions. *Miner. Eng.* **2018**, *116*, 35–45.
- (30) Faris, N.; White, J.; Magazowski, F.; Fischmann, A.; Jones, L. A.; Tardio, J.; Madapusi, S.; Grocott, S.; Bhargava, S. K. An investigation into potential pathways for nickel and cobalt loss during impurity removal from synthetic nickel laterite pressure leach solutions via partial neutralisation. *Hydrometallurgy* **2021**, *202*, 105595.
- (31) Pedrosa, J.; Costa, B. F. O.; Portugal, A.; Duraes, L. Controlled phase formation of nanocrystalline iron oxides/hydroxides in solution - An insight on the phase transformation mechanism. *Mater. Chem. Phys.* **2015**, *163*, 88–98.
- (32) Boland, D. D.; Collins, R. N.; Glover, C. J.; Waite, T. D. An in-situ quick EXAFS and redox potential study of the Fe(II) catalysed transformation of ferrihydrite. *Colloids Surf., A* **2013**, *435*, 2–8.
- (33) Liu, H.; Wei, Y.; Sun, Y. The formation of hematite from ferrihydrite using Fe(II) as a catalyst. *J. Mol. Catal. A: Chem.* **2005**, *226*, 135–140.
- (34) Cornell, R. M.; Schneider, W.; Giovanoli, R. Phase transformations in the ferrihydrite/cysteine system. *Polyhedron* **1989**, *8* (23), 2829–2836.
- (35) Andreeva, D.; Mitov, I.; Tabakova, T.; Mitrov, V.; Andreev, A. Influence of iron(II) on the transformation of ferrihydrite into goethite in acid medium. *Mater. Chem. Phys.* **1995**, *41*, 146–149.
- (36) Andreeva, D.; Mitov, I.; Tabakova, T.; Mitrov, V.; Andreev, A. Formation of goethite by oxidative hydrolysis of iron (II) sulphate. *J. Mater. Sci. Mater. Electron.* **1994**, *5*, 168–172.
- (37) Liu, H.; Chen, T.; Frost, R. L. An overview of the role of goethite surfaces in the environment. *Chemosphere* **2014**, *103*, 1–11.
- (38) Beukes, J. P.; Giesekke, E. W.; Elliott, W. Nickel retention by goethite and hematite. *Miner. Eng.* **2000**, *13*, 1573–1579.